DOI: 10.1002/chem.201101170

Lanthanide-Doped Multicolor GdF_3 Nanocrystals for Time-Resolved Photoluminescent Biodetection

Qiang Ju,[a, b] Yongsheng Liu,[a, b] Datao Tu,[a, b] Haomiao Zhu,[a, b] Renfu Li,[a, b] and Xueyuan Chen*[a, b]

The demand for precisely deciphering chemical information and simultaneous detection of multiple components of complex biomolecule assemblies (e.g., proteins, living cells) has driven the development of highly sensitive luminescent labeling.[1] The commonly used luminescent biolabels are grouped as lanthanide-based and non-lanthanide-based ones. Currently, non-lanthanide-based luminescent labeling generally relies on the use of organic dyes and quantum dots (QDs),[2] which might have some intrinsic limitations or drawbacks, such as photobleaching, spectrally overlapping between emission and excitation bands, broad emission band widths, and cytotoxicity. As an alternative to dyes and QDs, trivalent lanthanide ion (Ln^{3+})-doped nanocrystals (NCs) have been suggested as a promising new class of multicolor labeling, because they show more superior features, including narrow emission band widths (<10 nm), long luminescence lifetimes (μs-ms range), high photostability, and low toxicity.[3] Furthermore, conventional luminescent labeling, by means of steady-state detection, often suffers from the interferences of scattered lights and autofluorescence from cells and tissues, which result in a low signal-to-noise ratio (S/N). To completely eliminate such interferences and improve the detection sensitivity, the technique of time-resolved photoluminescent (TRPL), utilizing the long-lived luminescence of Ln^{3+} in the compounds such as commercial lanthanide-chelating agents, has been introduced in biomedical analyses.[4] In this way, the short-lived background luminescence is effectively suppressed when measuring the long-lived photoluminescence (PL) of Ln^{3+} by setting appropriate delay time and gate time, which thus offers a signal with remarkably high S/N (Figure 1). Because data sampling in the TRPL detection is completed in a few milliseconds, it can be repeated several thousand times during a minute,

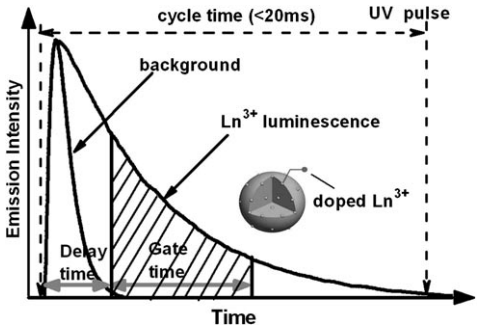

Figure 1. The principle of TRPL detection.

leading to a very high sensitivity within a few minutes.[5] However, the emissions of some Ln^{3+}-chelates may be quenched or significantly affected by solvents, such as water molecules or hydroxyl groups.[6] The concerns of the photostability and high cost of Ln^{3+}-chelating agents may, to some extent, limit the practical applications. By contrast, the Ln^{3+}-doped inorganic NCs, which possess rigid crystal lattices and provide a steady microenvironment for Ln^{3+} ions, have been proposed to be more photostable and economically beneficial for biolabeling. Despite the fact that Ln^{3+}-doped nanomaterials, such as Gd_2O_3:Ln^{3+} (Ln = Eu or Tb), LaF_3:Ln^{3+} (Ln = Eu, Tb or Nd), Ce^{3+}/Tb^{3+}-codoped $LaPO_4$, and Yb^{3+}/Tm^{3+} (or Er^{3+})-codoped $NaYF_4$ NCs, have been demonstrated occasionally in some biological analyses,[7] to the best of our knowledge, there is no report on Ln^{3+}-doped GdF_3 NCs integrated with the TRPL technique for luminescent biodetection.

The application of optical probes, however, is often limited by the low penetration depth of biological samples due to intrinsic tissue-signal attenuation. To compensate for such a deficiency, one strategy is to develop optical/magnetic dual-modal contrast agents, because magnetic resonance imaging (MRI) can provide excellent spatial resolution and depth.[8] Gd^{3+} ions—the best-known metal ion as a longitudinal relaxation time (T_1)-MRI contrast agent, thus far—have been extensively doped into luminescent NCs to enhance the MRI quality.[9] Moreover, Gd^{3+} may act as an efficient UV sensitizer to transfer the absorbed energy and activate other Ln^{3+} in proximity, which then exhibit multicolor emissions.[10] Consequently, Ln^{3+}-doped Gd^{3+}-containing NCs can serve as both multicolor luminescent biolabels and

[a] Dr. Q. Ju, Dr. Y. Liu, D. Tu, Dr. H. Zhu, R. Li, Prof. Dr. X. Chen
Key Laboratory of Optoelectronic Materials Chemistry and Physics
Fujian Institute of Research on the Structure of Matter
Chinese Academy of Sciences, Fuzhou, Fujian 350002 (China)
Fax: (+86) 591-8764-2575
E-mail: xchen@fjirsm.ac.cn

[b] Dr. Q. Ju, Dr. Y. Liu, D. Tu, Dr. H. Zhu, R. Li, Prof. Dr. X. Chen
State Key Laboratory of Structural Chemistry
Fuzhou, Fujian 350002 (China)

Supporting information for this article, including detailed experimental procedures, is available on the WWW under http://dx.doi.org/10.1002/chem.201101170.

MRI contrast agents. Herein, multicolor emissions that cover a wide range of colors under single-wavelength excitation have been achieved in GdF_3:Ln^{3+} (Ln = Eu, Tb, and Dy) NCs through the variation of both emitter combinations and dopant concentrations. By combining with the TRPL technique, we demonstrated the use of GdF_3:Ln^{3+} NCs as sensitive luminescent biolabels for the detection of avidin protein with a detection limit in the order of tens of pM. The positive contrast enhancement induced by GdF_3 NCs was also verified in T_1-MRI experiments.

Ln^{3+}-doped GdF_3 NCs were synthesized through a modified one-step solvothermal route.[7c,11] Poly(acrylic acid) (PAA, MW = 1800) was chosen as the capping agent to control the growth of NCs, and endow these NCs with water-solubility and biocompatibility (Figure S1 in the Supporting Information). The presence of capping PAA on the surfaces of NCs can be established by FTIR (Figure S2 in the Supporting Information). A strong IR band centered at 1721 cm^{-1} is observed, which can be attributed to the C=O stretching mode of protonated carboxylate groups (COOH) of PAA, thereby revealing the PAA capping on the NCs.[12] The ζ potential for the NC colloidal solution was measured to be −18.4 mV, which indicates negatively charged PAA on the surfaces of the NCs (Figure S3 in the Supporting Information). This result is further confirmed by the same decomposition temperature, starting at 200 °C, as revealed from thermogravimetric-analysis (TGA) curves for NCs and pure PAA (Figure S4 in the Supporting Information). Thanks to the carboxyl groups capping on the NC surface, the GdF_3 NCs can be steadily dispersed in water to form a transparent solution (Figure S5 in the Supporting Information). The as-prepared solution remains very stable in air for more than a month and no precipitate or aggregate was observed. Moreover, the NC solution is also very stable in NaCl solution (≤300 mM) and under different pH conditions (5–12), showing that the GdF_3:Ln^{3+} NC solution could withstand various biological conditions.[8c] TEM images shows that the as-prepared GdF_3:Tb^{3+} NCs are mainly composed of grainlike structures with a size that ranges from 30 to 50 nm (Figure S5 in the Supporting Information). The corresponding high-resolution TEM (HRTEM) image clearly demonstrates the high crystallinity of the GdF_3 NCs (Figure S6 in the Supporting Information). Lattice fringes are very clear with an observed d spacing of 0.361 nm, which is in good agreement with the lattice spacing for the (101) plane of the orthorhombic GdF_3 phase. The crystalline phase of the NCs can be further confirmed by the XRD analysis (Figure S6 in the Supporting Information). All the XRD patterns for the GdF_3 NCs can be exclusively indexed to the pure, orthorhombic-phase GdF_3 (JCPDS 049-1804), indicating the presence of the highly crystalline GdF_3 NCs without any other impurities. Composition analyses by energy dispersive X-ray spectroscopy (EDS) reveal the presence of Gd, F, and doped Ln ions for all GdF_3:Ln^{3+} NCs (Figure S7 in the Supporting Information).

As a proof-of-concept experiment, Eu^{3+}, Tb^{3+}, and Dy^{3+} ions were chosen as the emitters to generate desirable multicolor outputs in the GdF_3 NCs (Figure S8 in the Supporting Information). To demonstrate the feasibility of our strategy, PL excitation and emission spectra for Eu^{3+}, Tb^{3+}, and Dy^{3+} singly doped GdF_3 NCs (2.0 at.%) in aqueous solutions (Figure 2a) were measured at RT. By monitoring the

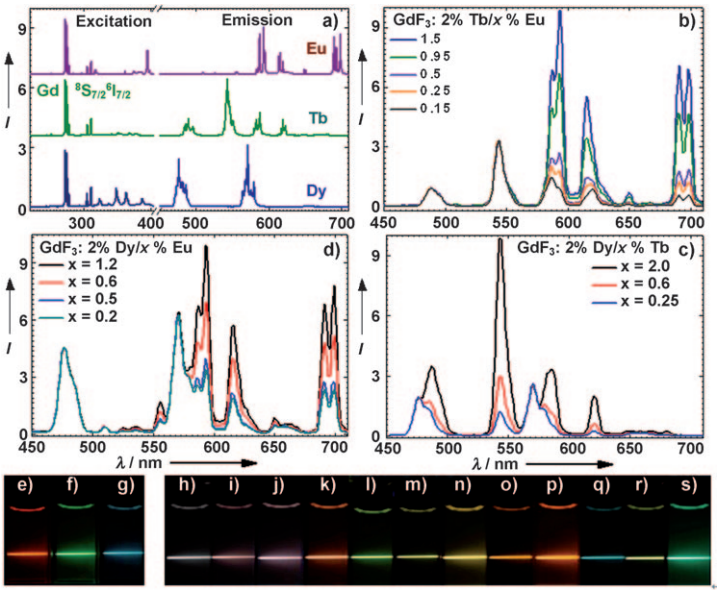

Figure 2. a) PL excitation and emission spectra for Eu^{3+}, Tb^{3+}, and Dy^{3+} singly doped GdF_3 (2.0 at.%) NCs in aqueous solutions. PL emission spectra of b) Eu^{3+} (x at.%)/Tb^{3+} (2.0 at.%), c) Tb^{3+} (x at.%)/Dy^{3+} (2.0 at.%), and d) Eu^{3+} (x at.%)/Dy^{3+} (2.0 at.%) doubly doped GdF_3 NCs. Compiled photographs showing the corresponding luminescence of Ln^{3+}-doped GdF_3 NCs in aqueous solutions e) GdF_3:Eu^{3+}(2.0 at.%), f) GdF_3:Tb^{3+}(2.0 at.%), g) GdF_3:Dy^{3+}(2.0 at.%), h–k) GdF_3:Eu^{3+}/Dy^{3+} (Dy = 2.0 at.%, Eu = 0.2, 0.5, 0.6, 1.2 at.%), l–p) GdF_3:Eu^{3+}/Tb^{3+} (Tb = 2.0 at.%, Eu = 0.15, 0.25, 0.5, 0.95, 1.5 at.%), q–s) GdF_3:Tb^{3+}/Dy^{3+} (Dy = 2.0 at.%, Tb = 0.25, 0.6, 2.0 at.%). The photographs are taken with an exposure time of 1.0 s, when the samples were irradiated with a 1 mW Ti:Sapphire third-harmonic-generation (THG) laser.

characteristic emissions of Eu^{3+}, Tb^{3+}, and Dy^{3+} at 593 ($^5D_0$→$^7F_1$), 543 ($^5D_4$→$^7F_5$), and 477 nm ($^4F_{9/2}$→$^6H_{15/2}$), respectively, the PL excitation spectra for Eu^{3+}, Tb^{3+}, and Dy^{3+} singly doped GdF_3 NCs were obtained. All the three excitation spectra are dominated by sharp excitation lines centered at 272 nm that correspond to the typical $^8S_{7/2}$→$^6I_{7/2}$ transitions of Gd^{3+}, suggesting that the Ln^{3+} emissions can be achieved through an energy-transfer process from the host to the Ln^{3+} dopants. Apart from the typical excitation lines of Gd^{3+}, much weaker excitation lines originating from Eu^{3+}, Tb^{3+}, and Dy^{3+} ions are also presented in Figure 2a, which proves that the host sensitization is a much more efficient pathway than the direct excitation of Ln^{3+} dopants in GdF_3 NCs. Upon excitation from the ground state, $^8S_{7/2}$ to $^6I_{7/2}$ of Gd^{3+} at 272 nm, intense and characteristic emission patterns of Eu^{3+}, Tb^{3+}, and Dy^{3+} are detected in the visible. These emission lines can be explicitly assigned to the $^5D_0$→$^7F_{0,1,2,3,4}$, $^5D_4$→$^7F_{6,5,4,3,2}$, and $^4F_{9/2}$→$^6H_{15/2,13/2,11/2}$ transitions for

Eu^{3+}, Tb^{3+}, and Dy^{3+} and thus resulted in red, green, and blue color outputs, respectively, without the use of any color filters. The corresponding PL photographs of the NC solutions are shown in Figures 2e–g. More importantly, the PL intensities of these NC solutions were found to remain unchanged after UV irradiation for 12 h, indicative of the high photostability of the NCs.

Multicolor emissions that span a wider spectral region can be easily achieved by varying the combination of emitters and molar ratios of different emitters. When codoping two types of Ln^{3+} ions with different ratios of concentration, the relative intensity of the dual Ln^{3+} emissions can be precisely controlled. To exemplify this, the emission spectra of GdF_3:Eu^{3+}/Tb^{3+} NCs with varied doping concentrations are exhibited in Figure 2b. Prior to doping with Eu^{3+}, the singly doped GdF_3:Tb^{3+} system exhibited green-color emission. By adding a second emitter (Eu^{3+}), of different concentrations, to the system, the relative intensity ratio of the dual emissions (Eu^{3+}/Tb^{3+}) can be finely tuned. As the concentration of Eu^{3+} varied from 0.15 to 1.5 at.%, while that of Tb^{3+} was fixed at 2.0 at.%, the PL intensity ratio of Eu^{3+}/Tb^{3+} markedly increased, giving rise to a color tuning from green to red (Figures 2l–p). The above concentration-dependent PL color tuning has also been applied to Tb^{3+}/Dy^{3+} and Eu^{3+}/Dy^{3+} doubly doped GdF_3 NCs, modulating their emission spectra by changing the concentration ratio of dual emitters (Figures 2c,d). As a result, their emission colors are tunable from red to orange, yellow, green, blue, purple, and white in turn (Figures 2q–s and Figures 2h–k for Tb^{3+}/Dy^{3+} and Eu^{3+}/Dy^{3+}, respectively).

To explore their potential applications in TRPL detection, we measured the PL lifetimes for Eu^{3+}, Tb^{3+}, and Dy^{3+} singly doped GdF_3 NCs (2.0 at.%) in aqueous solutions. The decay curves of Eu^{3+}, Tb^{3+}, and Dy^{3+} fit well to a single-exponential function, when monitoring their characteristic emissions at 593, 543, and 477 nm, respectively (Figure 3a). The PL lifetimes were determined to be 10.51, 5.91, and 0.86 ms for Eu^{3+}, Tb^{3+}, and Dy^{3+} singly doped NC samples, respectively. The distinct PL lifetime for various Ln^{3+} species in an identical host with the same doping concentration may be ascribed to differences in both nonradiative and radiative transition probabilities for the f–f transitions of Ln^{3+}, which are of forced electric–dipole or magnetic–dipole nature.[5] In comparison with multiexponential decay curves and a short PL lifetime (1.70 ms) of Eu^{3+} in recently reported GdF_3:Eu^{3+} nanoparticles (NPs),[13] the single-exponential decay and much longer PL lifetime of Eu^{3+} for the GdF_3:Eu^{3+} NCs in this work reveal that the doped Ln^{3+} ions reside in a more uniform and ordered crystalline environment. A similar long PL lifetime (11.0 ms) of Eu^{3+} in GdF_3:Eu^{3+} (0.5 at.%) NCs synthesized through a microwave reaction from ionic liquids were previously reported by Lorbeer et al.[10b] The PL lifetimes of Ln^{3+} in the codoped NCs show little variation compared with that of the singly doped counterparts. For example, the PL lifetimes were measured to be 10.81 and 5.83 ms for Eu^{3+} and Tb^{3+} in Eu^{3+} (0.5 at.%) and Tb^{3+} (2.0 at.%) codoped GdF_3 NCs,

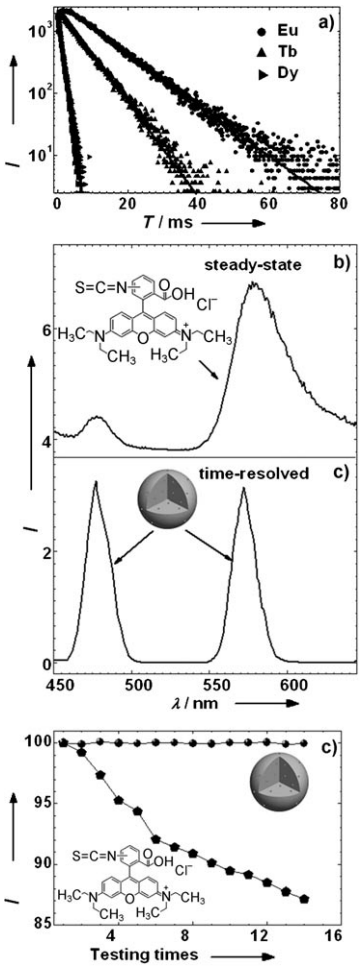

Figure 3. a) RT decay curves of Eu^{3+}, Tb^{3+}, and Dy^{3+} singly doped GdF_3 NCs (2.0 at.%) in aqueous solutions (1.0 mM) when monitoring by the emissions at 593, 543 and 477 nm, respectively. b) The steady-state and c) TRPL spectra of 0.1 mM GdF_3:Dy^{3+}(2.0 at.%) NCs mixed with 0.08 mM RBITC, respectively. d) The detection intensity of RBITC and GdF_3:Dy^{3+} as a function of observation times.

respectively. Although the cross energy transfer between codoped Ln^{3+} ions might occur, it has little influence on the lifetimes due to the fact that all Ln^{3+} ions are mainly populated through the energy transfer from Gd^{3+} ions as evidenced by the excitation spectra in Figure 2a.

Because of the long PL lifetime, the luminescence of Ln^{3+} is expected to be distinguished easily from the undesired short-lived background fluorescence of organic dyes, such as rhodamine B isothiocyanate (RBITC), by employing the TRPL detection. RBITC is chosen on purpose here as a typical source of short-lived background fluorescence, because its broad band emission (Figure S9 in the Supporting Information) partially overlaps with that of GdF_3:Ln^{3+}. The steady-state PL spectrum for the mixture of GdF_3:Dy^{3+} (0.1 mM) and RBITC (0.08 mM) is dominated by the emission of RBITC (Figure 3b). Emission bands from Dy^{3+} can hardly be observed due to the interference of the emission band from RBITC and scattered lights. In sharp contrast, only intense emission lines originating from Dy^{3+} were de-

tected in the TRPL spectrum when the delay time and gate time were set as 50 μs and 0.8 ms, respectively (Figure 3c). These results show unambiguously that the long-lived luminescence of Ln^{3+} combined with TRPL detection is particularly effective in removing undesired short-lived background fluorescence. Besides, as compared in Figure 3d, the PL intensity of RBITC under the steady-state detection gradually decreased as the testing times increased, whereas that of GdF_3:Dy^{3+} shows nearly no change under TRPL detection, indicating superior photostability of the GdF_3:Ln^{3+} NCs.

The application of GdF_3:Ln^{3+} NCs as sensitive TRPL probes was investigated in an avidin–biotin model system. The biotinylated NCs were prepared through a reported facile method (Figure S10 in the Supporting Information), in which NCs, dicyclohexylcarbodiimide (DCC), 1-hydroxybenzotriazole (HOBT), and biotin hydrazide were dissolved in DMF. The mixture was kept in an ultrasonic bath for two days at RT.[14] The successful attachment of biotin to the surface of the NCs was confirmed through FTIR spectra and the selective recognition of RBITC-labeled avidin for the NCs before and after bioconjugation. Two IR bands centered at 1208 and 1149 cm^{-1} as well as the distinguishable redshift of C=O (from 1721 to 1646 cm^{-1}) were observed for the biotinylated NC samples, which were assigned to the stretching modes of C–N from biotin and the substitution of amide for the protonated carboxylate group (Figure S2 in the Supporting Information). Upon incubation with the RBITC-labeled avidin, the emission spectrum of the biotinylated NC solution exhibited a significant increase in the PL signal of RBITC in contrast to the nonbiotinylated NCs (Figure S11 in the Supporting Information). Heterogeneous TRPL assays, which are commonly used to detect biomolecule analytes on a solid substrate and do not need strict control of the distance between biolabels and biomolecules, have been introduced into the detection of trace amounts of avidin captured on the microplate wells. The process for the heterogeneous TRPL assay (Figure 4a) was as follows: after coating different amount of avidin on the microplate wells, the same volume of a biotinylated NC solution (GdF_3:Tb^{3+}, 1 μg mL^{-1}) was added in each well and incubated for 3 h at RT, during which the biotinylated NCs were conjugated with avidin through a sensitive and specific interaction between avidin and biotin. The microplate was then washed several times and subjected to TRPL detection, and the analyte (avidin) could be quantified by measuring the PL intensity of the NCs bound to the wells. The observed TRPL signal was gradually enhanced with increasing amount of avidin bound to the well, thus quantitatively visualizing the binding between avidin and biotinylated NCs. The calibration curve of the TRPL detection for the concentration of avidin (Figure 4b) exhibits a nearly linear dependence in the concentration range of 1–100 ng mL^{-1} and tends to saturate when the concentration exceeds 100 ng mL^{-1}. The smaller slope in the saturation region may be due to the difficulty of keeping an equal binding efficiency between avidin and biotinylated NCs in view of the effect of steric hindrance among the relatively large NCs when the more

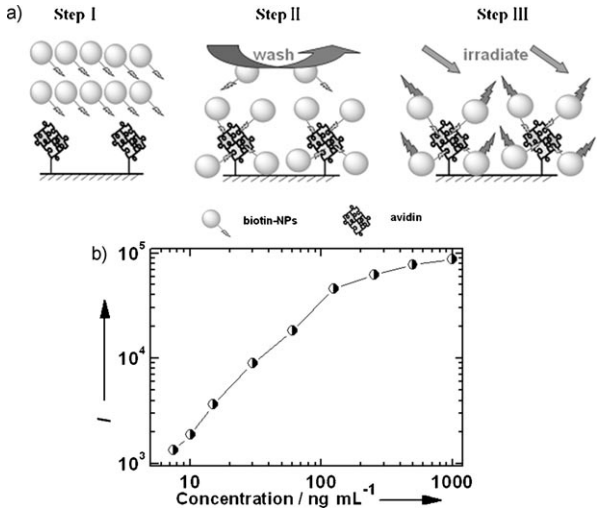

Figure 4. a) The process and principle of heterogeneous TRPL detection of avidin. b) Calibration curves of TRPL detection by employing biotinylated GdF_3:Tb^{3+} NCs as probes for the detection of avidin.

dense avidin molecules are coated on the well surface.[4e] The detection limit, defined as the concentration value that corresponds to three times as much as the standard deviation of the background signal, is 5 ng mL^{-1} (74 pM). Previously, Wang et al. reported a detection limit of ≈34 ng mL^{-1} (0.5 nM) for avidin by employing the fluorescence-resonant energy-transfer (FRET) method and $NaYF_4$ upconversion NPs as biolabels.[15] The detection sensitivity of the TRPL approach is approximately seven times higher than that of FRET.

To evaluate the potential application of GdF_3 NCs as MRI contrast agents, T_1 was measured in aqueous solutions with different Gd^{3+} concentrations. The longitudinal relaxivity (r_1) was estimated to be 1.44 s^{-1} mM^{-1} from the slope of the plot of $1/T_1$ versus the Gd^{3+} concentration (Figure 5a). The PAA capping on the NC surface could to some extent weaken the cooperative induction of surface Gd^{3+} ions for the longitudinal relaxation of a water proton.[16] It is anticipated that the r_1 value can be further improved through surface modifications, such as ligand engineering. Because a single NC contains many Gd^{3+} ions (more than 105 per NC), the GdF_3 NCs can provide a higher signal than single-molecule-based probes.[9a] In a proof-of-concept application as MRI contrast agents (Figure 5b), representative T_1-weighted magnetic resonance images of the NC suspensions clearly showed positive enhancement of the effect on T_1-weighted sequences as the NC concentration increased; this effect is comparable to that observed in commercial Gd–DPTA agents.[17] Previously, optical/magnetic dual-modal contrast agents were usually realized through the combination of QDs (or organic dyes) and superparamagnetic materials,[18] which involves rather complicated synthetic processes. Moreover, superparamagnetic NPs have several disadvantages, such as negative contrast effects and perturbation on normal tissues. Alternatively, the readily synthesized GdF_3:Ln^{3+} NCs may offer desirable dual-modality in which

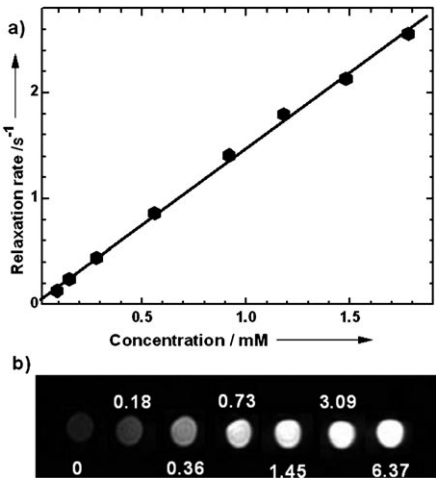

Figure 5. a) ^1H spin-lattice relaxation rates ($1/T_1$) of H_2O as a function of the molar concentration (mM) of GdF_3 NCs in a 4:1 (v/v) H_2O/D_2O mixture at RT and 9.4 T. b) T_1-weighted MRI of GdF_3 NCs at various concentrations in water (mM), showing clearly the positive enhancement effect on T_1-weighted sequences as the NC concentration increases.

the doped Ln^{3+} ions lead to long-lived multicolor luminescence for optical biolabeling and the Gd^{3+} ions from the host yield positive contrast effects for T_1 MRI.

In conclusion, we have synthesized water-soluble and carboxyl-group-enriched, Ln^{3+} (Eu^{3+}, Tb^{3+}, and Dy^{3+}) singly or multiply doped GdF_3 NCs through a facile one-step solvothermal route by employing PAA as the capping agent. By adjusting the combinations of Ln^{3+} dopants and doping concentrations, multicolor emissions that span a wide spectral region can be achieved in Ln^{3+}-doped GdF_3 NC solutions under single-wavelength excitation. When combined with the TRPL detection technique, the long-lived luminescence of the NCs allows for elimination of the interference of short-lived background and thus greatly enhances the S/N. The functionalized GdF_3 NCs have been demonstrated to be useful as TRPL probes to detect trace amounts of avidin protein and as robust MRI contrast agents. The GdF_3:Ln^{3+} NCs feature excellent water dispersibility and photostability, a broad color range under single-wavelength excitation, positive MRI contrast effects, absence of autofluorescence and low detection limits for TRPL detection, and thus are highly promising for versatile applications in time-resolved fluorometric immunoassays, multiplex detection, DNA hybridization, and dual-modality bioimaging.

Acknowledgements

This work is supported by the Hundred Talent Program of the Chinese Academy of Sciences (CAS), Knowledge Innovation Program of CAS for Key Topics (No. KJCX2-YW-358), the NSFC (Nos. 10974200 and 51002151), the 973 and 863 programs of MOST (Nos. 2007CB936703 and 2009AA03Z430), and the NSF of Fujian Province for Distinguished Young Scholars (Nos. 2009 J06030, 2009 J05138 and 2010 J05126).

Keywords: bioprobes · GdF_3 nanocrystals · lanthanides · magnetic resonance imaging · time-resolved photoluminescence

[1] a) W. C. W. Chan, S. M. Nie, *Science* **1998**, *281*, 2016; b) A. Miyawaki, *Dev. Cell* **2003**, *4*, 295; c) E. Schrock, S. du-Manoir, T. Veldman, B. Schoell, J. Wienberg, M. A. Ferguson-Smith, Y. Ning, D. H. Ledbetter, I. Bar-Am, D. Soenksen, Y. Garini, T. Ried, *Science* **1996**, *273*, 494; d) L. Wang, W. H. Tan, *Nano Lett.* **2006**, *6*, 84; e) L. Wang, C. Y. Yang, W. H. Tan, *Nano Lett.* **2005**, *5*, 37; f) M. De, P. S. Ghosh, V. M. Rotello, *Adv. Mater.* **2008**, *20*, 4225; g) F. Wang, X. G. Liu, *Chem. Soc. Rev.* **2009**, *38*, 976; h) F. Vetrone, R. Naccache, A. Zamarron, A. J. de La Fuente, F. Sanz-Rodriguez, L. M. Maestro, E. M. Rodriguez, D. Jaque, J. G. Sole, J. A. Capobianco, *ACS Nano* **2010**, *4*, 3254; i) F. Wang, D. Banerjee, Y. S. Liu, X. Y. Chen, X. G. Liu, *Analyst* **2010**, *135*, 1839; j) S. M. Borisov, O. S. Wolfbeis, *Chem. Rev.* **2008**, *108*, 423; k) M. V. Yezhelyev, A. Al-Hajj, C. Morris, A. I. Marcus, T. Liu, M. Lewis, C. Cohen, P. Zrazhevskiy, J. W. Simons, A. Rogatko, S. Nie, X. Gao, R. M. O'Regan, *Adv. Mater.* **2007**, *19*, 3146.

[2] a) C. D. Müller, A. Falcou, N. Reckefuss, M. Rojahn, V. Wiederhirn, P. Rudati, H. Frohne, O. Nuyken, H. Becker, K. Meerholz, *Nature* **2003**, *421*, 829; b) X. Michalet, F. F. Pinaud, L. A. Bentolila, J. M. Tsay, S. Doose, J. J. Li, G. Sundaresan, A. M. Wu, S. S. Gambhir, S. Weiss, *Science* **2005**, *307*, 538; c) M. Kuang, D. Y. Wang, H. B. Bao, M. Y. Gao, H. Mohwald, M. Jiang, *Adv. Mater.* **2005**, *17*, 267; d) K. Umezawa, Y. Nakamura, H. Makino, D. Citterio, K. Suzuki, *J. Am. Chem. Soc.* **2008**, *130*, 1550; e) M. Y. Han, X. H. Gao, J. Z. Su, S. Nie, *Nat. Biotechnol.* **2001**, *19*, 631; f) K. T. Yong, I. Roy, H. Ding, E. J. Bergey, P. N. Prasad, *Small* **2009**, *5*, 1997.

[3] a) M. J. Dejneka, A. Streltsov, S. Pal, A. G. Frutos, C. L. Powell, K. Yost, P. K. Yuen, U. Muller, J. Lahiri, *Proc. Natl. Acad. Sci. USA* **2003**, *100*, 389; b) S. M. Hussain, L. K. Braydich-Stolle, A. M. Schrand, R. C. Murdock, K. O. Yu, D. M. Mattie, J. J. Schlager, M. Terrones, *Adv. Mater.* **2009**, *21*, 1549; c) P. Ptacek, H. Schäfer, K. Kömpe, M. Haase, *Adv. Funct. Mater.* **2007**, *17*, 3843; d) F. Vetrone, V. Mahalingam, J. A. Capobianco, *Chem. Mater.* **2009**, *21*, 1847; e) F. Wang, Y. Han, C. S. Lim, Y. H. Lu, J. Wang, J. Xu, H. Y. Chen, C. Zhang, M. H. Hong, X. G. Liu, *Nature* **2010**, *463*, 1061; f) L. Y. Wang, Y. D. Li, *Chem. Eur. J.* **2007**, *13*, 4203; g) H. Schäfer, P. Ptacek, K. Kompe, M. Haase, *Chem. Mater.* **2007**, *19*, 1396; h) J. F. Liu, Y. D. Li, *Adv. Mater.* **2007**, *19*, 1118; i) F. Wang, X. J. Xue, X. G. Liu, *Angew. Chem.* **2008**, *120*, 920; *Angew. Chem. Int. Ed.* **2008**, *47*, 906; j) F. Wang, X. G. Liu, *J. Am. Chem. Soc.* **2008**, *130*, 5642; k) G. F. Wang, Q. Peng, Y. D. Li, *J. Am. Chem. Soc.* **2009**, *131*, 14200; l) G. S. Yi, G. M. Chow, *Adv. Funct. Mater.* **2006**, *16*, 2324; m) K. Kömpe, H. Borchert, J. Storz, A. Lobo, S. Adam, T. Möller, M. Haase, *Angew. Chem.* **2003**, *115*, 5672; *Angew. Chem. Int. Ed.* **2003**, *42*, 5513; n) Z. Q. Li, Y. Zhang, S. Jiang, *Adv. Mater.* **2008**, *20*, 4765; o) V. Mahalingam, F. Vetrone, R. Naccache, A. Speghini, J. A. Capobianco, *Adv. Mater.* **2009**, *21*, 4025; p) H. Schäfer, P. Ptacek, H. Eickmeier, M. Haase, *Adv. Funct. Mater.* **2009**, *19*, 3091; q) G. Y. Chen, T. Y. Ohulchanskyy, R. Kumar, H. Agren, P. N. Prasad, *ACS Nano* **2010**, *4*, 3163; r) F. Wang, J. A. Wang, X. G. Liu, *Angew. Chem.* **2010**, *122*, 7618; *Angew. Chem. Int. Ed.* **2010**, *49*, 7456; s) M, Haase, H. Schäfer, *Angew. Chem.* **2011**, *123*, 5928–5950; *Angew. Chem. Int. Ed.* **2011**, *50*, 5808–5829.

[4] a) N. Weibel, L. J. Charbonniere, M. Guardigli, A. Roda, R. Ziessel, *J. Am. Chem. Soc.* **2004**, *126*, 4888; b) B. Song, G. L. Wang, M. Q. Tan, J. L. Yuan, *J. Am. Chem. Soc.* **2006**, *128*, 13442; c) K. Hanaoka, K. Kikuchi, S. Kobayashi, T. Nagano, *J. Am. Chem. Soc.* **2007**, *129*, 13502; d) D. Geißler, L. J. Charbonniere, R. F. Ziessel, N. G. Butlin, H. G. Lohmannsroben, N. Hildebrandt, *Angew. Chem.* **2010**, *122*, 1438; *Angew. Chem. Int. Ed.* **2010**, *49*, 1396; e) Z. Q. Ye, M. Q. Tan, G. L. Wang, J. L. Yuan, *Anal. Chem.* **2004**, *76*, 513; f) H. E. Rajapakse, D. R. Reddy, S. Mohandessi, N. G. Butlin, L. W. Miller, *Angew. Chem.* **2009**, *121*, 5090; *Angew. Chem. Int. Ed.* **2009**, *48*,

4990; g) G. L. Law, K. L. Wong, C. W. Y. Man, W. T. Wong, S. W. Tsao, M. H. W. Lam, P. K. S. Lam, *J. Am. Chem. Soc.* **2008**, *130*, 3714.

[5] a) J. C. G. Bünzli, *Chem. Lett.* **2009**, *38*, 104; b) J. C. G. Bünzli, *Chem. Rev.* **2010**, *110*, 2729; c) J. C. G. Bünzli, C. Piguet, *Chem. Soc. Rev.* **2005**, *34*, 1048.

[6] a) Y. Chen, Y. M. Chi, H. M. Wen, Z. H. Lu, *Anal. Chem.* **2007**, *79*, 960; b) J. Shen, L. D. Sun, C. H. Yan, *Dalton Trans.* **2008**, 5687; c) K. L. Ai, B. H. Zhang, L. H. Lu, *Angew. Chem.* **2009**, *121*, 310; *Angew. Chem. Int. Ed.* **2009**, *48*, 304.

[7] a) C. Louis, R. Bazzi, C. A. Marquette, J. L. Bridot, S. Roux, G. Ledoux, B. Mercier, L. Blum, P. Perriat, O. Tillement, *Chem. Mater.* **2005**, *17*, 1673; b) P. R. Diamente, R. D. Burke, F. C. J. M. van Veggel, *Langmuir* **2006**, *22*, 1782; c) J. Q. Gu, J. Shen, L. D. Sun, C. H. Yan, *J. Phys. Chem. C* **2008**, *112*, 6589; d) S. Sivakumar, P. R. Diamente, F. C. van Veggel, *Chem. Eur. J.* **2006**, *12*, 5878; e) L. Y. Wang, Y. D. Li, *Chem. Commun.* **2006**, 2557; f) F. Vetrone, R. Naccache, A. J. de La Fuente, F. Sanz-Rodriguez, A. Blazquez-Castro, E. M. Rodriguez, D. Jaque, J. G. Sole, J. A. Capobianco, *Nanoscale* **2010**, *2*, 495.

[8] a) H. B. Na, I. C. Song, T. Hyeon, *Adv. Mater.* **2009**, *21*, 2133; b) C. Tu, R. Nagao, A. Y. Louie, *Angew. Chem.* **2009**, *121*, 6669; *Angew. Chem. Int. Ed.* **2009**, *48*, 6547; c) Y. M. Huh, Y. W. Jun, H. T. Song, S. Kim, J. S. Choi, J. H. Lee, S. Yoon, K. S. Kim, J. S. Shin, J. S. Suh, J. Cheon, *J. Am. Chem. Soc.* **2005**, *127*, 12387; d) K. T. Yong, I. Roy, M. T. Swihart, P. N. Prasad, *J. Mater. Chem.* **2009**, *19*, 4655.

[9] a) F. Evanics, P. R. Diamente, F. C. J. M. van Veggel, G. J. Stanisz, R. S. Prosser, *Chem. Mater.* **2006**, *18*, 2499; b) R. Kumar, M. Nyk, T. Y. Ohulchanskyy, C. A. Flask, P. N. Prasad, *Adv. Funct. Mater.* **2009**, *19*, 853; c) Y. Park, J. H. Kim, K. T. Lee, K. S. Jeon, H. Bin Na, J. H. Yu, H. M. Kim, N. Lee, S. H. Choi, S. I. Baik, H. Kim, S. P. Park, B. J. Park, Y. W. Kim, S. H. Lee, S. Y. Yoon, I. C. Song, W. K. Moon, Y. D. Suh, T. Hyeon, *Adv. Mater.* **2009**, *21*, 4467; d) W. J. Rieter, J. S. Kim, K. M. L. Taylor, H. Y. An, W. L. Lin, T. Tarrant, W. B. Lin, *Angew. Chem.* **2007**, *119*, 3754; *Angew. Chem. Int. Ed.* **2007**, *46*, 3680; e) H. Hifumi, S. Yamaoka, A. Tanimoto, D. Citterio, K. Suzuki, *J. Am. Chem. Soc.* **2006**, *128*, 15090; f) Y. S. Liu, D. T. Tu, H. M. Zhu, R. F. Li, W. Q. Luo, X. Y. Chen, *Adv. Mater.* **2010**, *22*, 3266.

[10] a) P. A. Tanner, J. W. Wang, *Chem. Phys. Lett.* **2008**, *455*, 335; b) C. Lorbeer, J. Cybinska, A. V. Mudring, *Chem. Commun.* **2010**, *46*, 571.

[11] Q. Ju, W. Q. Luo, Y. S. Liu, H. M. Zhu, R. F. Li, X. Y. Chen, *Nanoscale* **2010**, *2*, 1208.

[12] T. R. Zhang, J. P. Ge, Y. P. Hu, Y. D. Yin, *Nano. Lett.* **2007**, *7*, 3203.

[13] C. H. Dong, F. C. J. M. van Veggel, *ACS Nano* **2009**, *3*, 123.

[14] G. T. Hermanson, *Bioconjugate Techniques*, Academic Press, New York, **1996**.

[15] L. Y. Wang, R. X. Yan, Z. Y. Hao, L. Wang, J. H. Zeng, H. Bao, X. Wang, Q. Peng, Y. D. Li, *Angew. Chem.* **2005**, *117*, 6208; *Angew. Chem. Int. Ed.* **2005**, *44*, 6054.

[16] J. Y. Park, M. J. Baek, E. S. Choi, S. Woo, J. H. Kim, T. J. Kim, J. C. Jung, K. S. Chae, Y. Chang, G. H. Lee, *ACS Nano* **2009**, *3*, 3663.

[17] J. Zhou, Y. Sun, X. X. Du, L. Q. Xiong, H. Hu, F. Y. Li, *Biomaterials* **2010**, *31*, 3287.

[18] a) J. Kim, H. S. Kim, N. Lee, T. Kim, H. Kim, T. Yu, I. C. Song, W. K. Moon, T. Hyeon, *Angew. Chem.* **2008**, *120*, 8566; *Angew. Chem. Int. Ed.* **2008**, *47*, 8438; b) X. Zhang, M. Brynda, R. D. Britt, E. C. Carroll, D. S. Larsen, A. Y. Louie, S. M. Kauzlarich, *J. Am. Chem. Soc.* **2007**, *129*, 10668; c) R. Kumar, I. Roy, T. Y. Ohulchanskky, L. A. Vathy, E. J. Bergey, M. Sajjad, P. N. Prasad, *ACS Nano* **2010**, *4*, 699.

Received: April 16, 2011
Published online: June 15, 2011

